Water Research X 9 (2020) 100059

Contents lists available at ScienceDirect

Water Research X

journal homepage: https://www.journals.elsevier.com/water-research-x

Quantification of anthropogenic and geogenic Ce in sewage sludge based on Ce oxidation state and rare earth element patterns

Alexander Gogos [a, b], Jonas Wielinski [a, c], Andreas Voegelin [a], Frank von der Kammer [d], Ralf Kaegi [a, *]

[a] Eawag, Swiss Federal Institute of Aquatic Science and Technology, Überlandstrasse 133, CH-8600, Dübendorf, Switzerland
[b] EMPA, Swiss Federal Laboratories for Materials Science and Technology, 9014, St. Gallen, Switzerland
[c] ETH Zürich, Institute of Environmental Engineering, 8093, Zürich, Switzerland
[d] University of Vienna, Department of Environmental Geosciences and Environmental Science Research Network, Althanstr. 14, UZA II, 1090, Vienna, Austria

ARTICLE INFO

Article history:
Received 13 March 2020
Accepted 2 July 2020
Available online 3 July 2020

Keywords:
Engineered nanoparticles
Cerium
X-ray absorption spectroscopy
Wastewater
Biosolids

ABSTRACT

Emissions of Ce from anthropogenic activities (anthropogenic Ce) into urban wastewater systems and the environment result from its widespread industrial use (abrasives, catalysts, nanotechnology). Because Ce in sewage sludge can also be of geogenic origin, the quantification of anthropogenic Ce in sewage sludge remains elusive. In this study, we evaluated the suitability of Ce oxidation state and rare earth element (REE) patterns for the quantification of anthropogenic Ce fractions in sewage sludge. A diverse set of soil samples served to gain baseline information on geogenic Ce. Geogenic Ce in the soils was characterized by high Ce(III) fractions (≥70%) and their REE patterns were comparable to the REE patterns of the upper continental crust. The sewage sludges contained on average ~80% Ce(IV) (range 18–108%), pointing to the importance of anthropogenic inputs of Ce(IV). The quantification of the anthropogenic Ce fraction based on Ce oxidation state, however, was associated with considerable uncertainty because geogenic and anthropogenic Ce cannot exclusively be assigned to Ce(III) and Ce(IV), respectively. The REE patterns of most sewage sludges indicated a clear enrichment of Ce compared to heavier REE. Based on the assumption that the industrially used Ce is free of (most) other REE, we estimated the fraction of anthropogenic Ce in the sludges based on individual Ce/REE ratios. For the individual sludges the anthropogenic contributions were very variable (10–100%) but consistent fractions were obtained for individual sludges when calculated based on Ce/Dy (dysprosium), Ce/Er (erbium) and Ce/Eu (europium) ratios. Electron microscopy analysis of sludges dominated by anthropogenic Ce revealed that the Ce was mostly contained in nanoscale particles devoid of elements characteristic of Ce-bearing minerals. Thus, anthropogenic Ce contents derived from REE patterns may be used to validate current mass flow models for engineered CeO_2 nanoparticles.

1. Introduction

Cerium (Ce) is the most abundant element among the rare earth elements (REE) (Henderson, 2013). In the environment, most REE are exclusively present in the trivalent state, but Ce may also occur in the tetravalent state (Marcus et al., 2018; Takahashi et al. 2000, 2002, 2005). Cerium (III), resulting from weathering of rocks, can precipitate as Ce(IV) under oxidizing conditions, resulting in a distinct transport, fractionation and enrichment behaviour of Ce compared to other REE, which is referred to as the Ce-anomaly (Henderson, 2013). However, in terrestrial systems, Ce occurs mainly as Ce(III) in accessory minerals of igneous rocks, such as phosphates, silicates, carbonates and oxides (Dahle and Arai, 2015; Henderson, 2013; Kabata-Pendias, 2010; Schreiber et al., 1980).

For industrial uses, Ce is extracted mostly from the minerals bastnaesite ($Ce(CO_3)F$) and monazite ($CePO_4$) and separated from other REE by oxidation to Ce(IV) and precipitation as ceria ($Ce(IV)O_2$). Hence, $Ce(IV)O_2$ is considered the most widely industrially used Ce compound (Voncken, 2016). The industrial use of Ce in catalysts (e.g., in fluid catalytic cracking of hydrocarbons, automotive catalysts), abrasives (chemical-mechanical planarization (CMP)), additives (glass production) and alloys (Mischmetall) (Voncken, 2016)

* Corresponding author.
E-mail address: ralf.kaegi@eawag.ch (R. Kaegi).

https://doi.org/10.1016/j.wroa.2020.100059

results in the emission of Ce. Over the last two decades, also an increasing number of applications of nanoscale CeO_2 have been developed, especially as catalyst and CMP agent. However, anthropogenic activities can also emit geogenic Ce, e.g., mining via acid mine drainage (Merten and Büchel, 2004) or the burning of coal (Kabata-Pendias, 2010). In this work, we therefore use the term "anthropogenic Ce" to refer to "anthropogenic Ce emitted from industrial/commercial Ce applications" unless stated otherwise.

Wastewater treatment plants (WWTP) efficiently remove particulate matter from the wastewater stream, which in turn leads to an accumulation of the respective material in the sewage sludge. Therefore, anthropogenic Ce discharged to municipal sewer systems is mixed with geogenic Ce inputs resulting for example from surface run-off (including eroded soil material) or extraneous water (or mine drainage). Cerium contents in sewage sludge from WWTP have been quantified in several studies. Cerium concentrations of up to 153 mg kg^{-1} were reported from the UK and were attributed to inputs from the glass industry (Vivian, 1986). More recently, a monitoring study of three WWTP in China (Suanon et al., 2017) and a survey of the metal contents in sewage sludge from Switzerland (Vriens et al., 2017) revealed that sewage sludge can contain up to $\approx$800 mg kg^{-1} Ce in the total suspended solids (TSS). The median Ce content of municipal sewage sludge from Switzerland ($\approx$20 mg kg^{-1}; n = 64), however, was below its average crustal abundance (60 mg kg^{-1} (Voncken, 2016)). Thus, elevated Ce concentrations (>100 mg kg^{-1}) clearly point to industrial Ce inputs.

The ability to discriminate between geogenic and anthropogenic Ce is crucial for the assessment of potential environmental impacts of anthropogenic Ce as well as for our understanding of global Ce mass flows. Based on the notion that industrial applications of Ce mainly result in emission of Ce(IV)(O_2) and geogenic Ce is mainly Ce(III) (Henderson, 2013; Voncken, 2016), we hypothesize that the oxidation state of Ce in sewage sludge can be used to quantify the fractions of Ce of anthropogenic and geogenic origin. Trivalent Ce in natural Ce-bearing minerals such as monazite and allanite, occurs together with other REE, whereas industrial CeO_2 (nano-) particles are expected to contain only negligible amounts of impurities (Laycock et al., 2016). Based on a consistent Ce:La ratio of $\approx$2:1 observed in soils worldwide (Ce:La based on world average ~ 1.9) (Kabata-Pendias, 2010) the Ce:La ratios were recently suggested as a proxy to identify anthropogenic Ce inputs into natural environments (Praetorius et al., 2017). We therefore hypothesize that the ratio of Ce over La and over other REE can be used to identify and eventually quantify anthropogenic Ce inputs into wastewater systems.

In this study, we evaluated to which extent the oxidation state of Ce and Ce:REE ratios can be used to identify and quantify anthropogenic Ce inputs into WWTP systems. A suite of sewage sludge samples were investigated that cover a wide range of Ce concentrations (10–1111 mg kg^{-1}) and potentially variable anthropogenic and geogenic Ce fractions. Using Ce L_{III}-edge X-ray absorption near-edge structure (XANES) spectroscopy, the fractions of Ce(III) and Ce(IV) in sewage sludge samples and in soil samples (as proxies for geogenic Ce) were quantified. In addition, Ce:REE ratios were determined in total digests using inductively coupled plasma mass spectrometry (ICP MS) and used to estimate the fraction of anthropogenic Ce. Finally, analytical electron microscopy was employed to distinguish between natural and anthropogenic Ce particles and to assess the size fraction in which (anthropogenic) Ce particles dominantly occur.

2. Materials and methods

2.1. Soil samples

Soil samples were obtained from the Swiss Soil Monitoring Network (Nationale Bodenbeobachtung, NABO, 2019). All samples originated from the 3rd collection, which was performed during the year 1995 (Desaules et al., 2006). Three samples were selected to represent different land uses in differently industrialized areas: NABO Soil 53 (So1) was collected from a pasture in Gempen (Canton Solothurn) located $\approx$3 km south of an industrial zone (Muttenz/Pratteln, Canton Basel Landschaft) and east of metal works (Reinach/Dornach, Canton Basel Landschaft) as well as a residential neighborhood. NABO Soil 62 (So2) was collected from a forest in Bettlach (Canton Solothurn) located $\approx$3 km from a general residential neighborhood. NABO Soil 103 (So3) originates from an agricultural area in Härkingen (Canton Solothurn) in $\approx$15 m distance to a highway. The sample locations are given in the SI (Fig. S1) and in (Desaules et al., 2006).

Furthermore, the reference soils ISE 950 (sandy soil from Tanzania, So4) and ISE 858 (pseudo-gleyic brown-earth from Zurich, Switzerland, So5) were obtained from WEPAL (Wageningen evaluating programs for analytical laboratories, Wageningen, The Netherlands). Finally, So6 was obtained from a previous study (Praetorius et al., 2017). All soil characteristics are given in Table S1.

2.2. Collection of sewage sludge samples

Anaerobically digested sewage sludge was collected at the Swiss WWTPs of Yverdon-les-Bains (SLG1, Canton Vaud, mixed industrial and municipal wastewater), St. Gallen (SLG2, Canton St. Gallen, municipal wastewater), Hofen (SLG3, Canton St. Gallen, municipal wastewater), Buchs (SLG4, Canton St. Gallen, municipal wastewater), and Basel (SLG5, Canton Basel-Stadt, mixed industrial and municipal wastewater) (Fig. S2 and Table S2). The sludge samples were freeze-dried and ground in a ball mill (MM200, Retsch GmbH, Haan, Germany; 4 min at 17 Hz). Sludge samples SLG1 and SLG2 were collected during the course of a previous study, which was focused on total metal contents in Swiss wastewaters (Vriens et al., 2017). Additionally, an industrial sludge from New Jersey, USA (SLG6, SRM 2782, effluent from an industrial site with pharmaceutical research, collected before treatment, National Institute of Standards and Technology (NIST), Gaithersburg, USA) was included due to its industrial origin and its high Ce concentration (reference value of 1240 mg Ce kg^{-1}).

2.3. Characterization of soils and sewage sludge

2.3.1. Total REE contents

The total contents of Ce, lanthanum (La), europium (Eu), dysprosium (Dy) and erbium (Er) (representing light, medium and heavy REE) in the dry sludge and soil were determined by digesting $\approx$20–30 mg of the ground material in a mixture of 7 mL HNO_3, 1 mL H_2O_2 and 0.1 mL HF in a microwave (MLS ultraCLAVE, MLS GmbH, Leutkirch, Germany). Digested samples were filled up to 50 mL with nanopure water and analyzed using ICP MS (Agilent 8900, Agilent Technologies Inc, CA, USA). For quality assurance, SLG6 (NIST SRM 2782, reference concentration of 1240 mg Ce kg^{-1}, 58.1 mg La kg^{-1} and an informational value of 0.34 mg Eu kg^{-1}) and a soil reference material (ISE 884, WEPAL, Wageningen, The Netherlands, reference concentration of 52.6 mg kg^{-1} Ce and 26 mg kg^{-1} La) were digested and analyzed along with the samples. The recovery for Ce, La and Eu was 90%, 88% and 85%, respectively for the industrial sludge. For the soil, a recovery for Ce and La of 103 and 94% was achieved. All samples were analyzed in triplicates. All concentrations (soils and sludges) for Ce and the other REE are tabulated (Table S3).

2.3.2. X-ray absorption spectroscopy (XAS)

Samples were measured at the Ce L_{III}-edge (5723 eV) at the

SuperXAS (X10DA) beamline at the Swiss Light Source (SLS, Villigen, Switzerland). The samples were prepared as pellets by mixing 90 mg of the dry and ball milled sample with 4 mg boron carbide and 4 mg quartz sand in an agate mortar and subsequent mixing with 10 mg cellulose. From this mixture, 80 mg were pressed into a 7 mm pellet using a handheld press. During the measurements, all samples and references were cooled with a N_2 gas stream set to 100 K using a CryoJet (Oxford Instruments). The energy of the X-ray beam was calibrated by setting the first inflection point of the Ce-L_{III}-edge spectrum of Ce(IV)O_2 to 5723 eV. All sample spectra and reference spectra of (bulk-) Ce(IV)O_2 and Ce(III)-allanite were measured in fluorescence mode using a 5-element silicon drift detector (SGX Sensortech, Buckinghamshire, UK). The structure of the reference materials has previously been confirmed by X-ray diffraction (Gogos et al., 2019).

The software code SIXPack (Webb, 2005) was used to process the XAS data following standard procedures to quantify the different Ce species by linear combination fit (LCF) analysis. For LCF analysis, the XANES data between 5703 and 5843 eV were evaluated. The fractions of individual Ce species in the LCF analysis were constrained to values between 0 and 1, but the sum of the fractions was not constrained. Due to interferences at the La L_{II} edge (5891 eV), the EXAFS data were not evaluated.

2.3.3. Electron microscopy

Samples for electron microscopy (EM) analyses were prepared by dispersing 15 mg of powdered sample in 1.5 mL 0.2% NovaChem (Postnova GmbH, Landsberg, Germany) using ultrasonication for 5 min (10 s ON and 20 s OFF, 200 W, amplitude of 100%, Vial Tweeter, Hielscher Ultrasonics GmbH, Germany). The resulting dispersion was diluted 1:100 in 0.02% NovaChem and centrifuged onto a 0.1% poly-L-lysine functionalized carbon Cu grid (EM Resolutions Ltd, Sheffield, UK) at 14,000 g for 1 h. Subsequently, the grids were washed three times in a drop of nanopure water and air dried. Electron microscopy images were recorded on a scanning transmission electron microscope (STEM, HD-2700-Cs, Hitachi, Japan) at an accelerating voltage of 200 kV using either a secondary electron (SE) or a high-angle annular dark field (HAADF) detector.

3. Results and discussion

3.1. Ce oxidation state in soils

The Ce L_{III}-edge XANES spectra of soil samples showed a clear Ce(III) signature at 5727 eV (Fig. 1 A, dashed line), comparable to the Ce-allanite reference. However, except for soil So6, each spectrum also showed a slightly increased shoulder at 5739 eV (Fig. 1 A, right dotted line), which is a characteristic feature for Ce(IV).

These observations were substantiated by LCF analyses (Fig. 1 B and Table S4). As the Ce L_{III}-XANES is more sensitive to Ce oxidation state than structural variations (especially for Ce(III) species (Takahashi et al., 2002)), we only used Ce-allanite and Ce(IV)O_2 as references to quantify the fractions of Ce(III) and Ce(IV) by LCF. The inclusion of further reference spectra of Ce(III)-parisite or Ce(III)PO_4 (Gogos et al., 2019) did not improve fit quality.

In general, the redox speciation of Ce in soils was dominated by Ce(III) regardless of the soil type, with Ce(IV) fractions of up to ≈ 30%. On average, the topsoil samples contained ≈84 ± 15% Ce(III) and 18 ± 11% Ce(IV) (±one standard deviation over all soil samples, Table S4), in good agreement with a XANES study returning 88–90% Ce(III) in the top 50 cm of a paddy soil (Takahashi et al., 2005).

3.2. Ce oxidation state in sewage sludge

The XANES spectra of the sludges SLG1 to SLG3 were almost identical to the spectrum of the Ce(IV)O_2 reference indicated by the two characteristic oscillations at 5732 and 5739 eV (Ce(IV), dotted lines) (Fig. 1 A). Furthermore, in the spectra of SLG1 and SLG3 the characteristic feature for Ce(III) (oscillation at 5727 eV) was lacking, suggesting that – within the uncertainty of the method - Ce in these sludges was exclusively Ce(IV). Sludge SLG2, however, showed a pronounced shoulder at 5727 eV, indicating the presence of Ce(III). The sludges SLG4 and SLG5 also showed features characteristic of both Ce(III) and Ce(IV). Quantitative LCF results confirmed these qualitative interpretations (Fig. 1 B and Table S4). With the exception of SLG6, LCF analysis of all sludge spectra returned higher Ce(IV) fractions compared to the soil spectra. Based on the assumption that anthropogenic Ce is dominated by Ce(IV), its input into wastewater should be accompanied by an increase in Ce(IV) in the sewage sludge. However, there was no apparent correlation between Ce contents and the Ce(IV) fractions (Fig. 2 A), indicating that Ce oxidation state alone is not sufficient to assess anthropogenic Ce inputs.

3.3. Ce:La ratios and rare earth element patterns

3.3.1. Ce:La ratios

The Ce:La ratios of soils and sludges were distinctly different (Fig. 1 C): Whereas soils had an average Ce:La ratio of 2.1 ± 0.3, the Ce:La ratios in the sludges were much higher (10.6 ± 6.5 for SLG1 to SLG4 and SL6), except for SLG5 (Ce:La = 1.1), pointing to anthropogenic Ce inputs. If anthropogenic Ce inputs were dominated by Ce(IV) and free of La, a positive correlation between the Ce(IV) fraction and the Ce:La ratio would be observable. However, the Ce:La ratio was not well correlated to the Ce oxidation state (Fig. 2 B). This is most evident, when comparing the Ce oxidation state and the Ce:La ratio of SLG1 and SLG6: although the Ce concentrations and Ce:La ratios of these two sludges were high, the Ce(IV) fractions were 100% and 18%, respectively. A possible explanation for these considerable variabilities are individual point sources discharging either (particulate) Ce(IV) or Ce(III) into the wastewater. Possible anthropogenic sources of Ce(III) include for example the glass industry (Darab et al., 1998), but also pharmaceutical research and industry (Martin et al., 1988). The latter one is most likely responsible for the high Ce(III) fractions observed in SLG6. Furthermore, possible anthropogenic emissions of La may additionally modify the Ce:La ratio. This is supported by Fig. 2 C: An increase in anthropogenic Ce inputs should lead to a corresponding increase of the Ce:La ratio if anthropogenic Ce is free of La. However, the Ce:La ratio of the sludges did not scale with the Ce concentration. For example, SLG3 showed a comparatively low Ce:La ratio but a rather high Ce concentration (181 mg kg^{-1}), pointing to anthropogenic La inputs. As recently described by Kulaksız and Bau (2011), such anthropogenic La inputs affect the Ce:La ratio and thus hamper the quantification of anthropogenic Ce fractions based on Ce:La ratios.

3.3.2. Rare earth element patterns

Rare earth elements other than La may be more suitable for the quantification of anthropogenic Ce in sewage sludge as they are much less used than La (Haque et al., 2014). We therefore investigated whether the contents of the REE Eu, Dy and Er, representing medium and heavy REE, allow for a more reliable identification and quantification of the anthropogenic Ce in sewage sludge. For that purpose, the contents of the REE in the sludges and soils were normalized over their contents in Post-Archean Australian Shale (PAAS), which represents the average upper continental crust (Pourmand et al., 2012). The resulting REE patterns of soils were

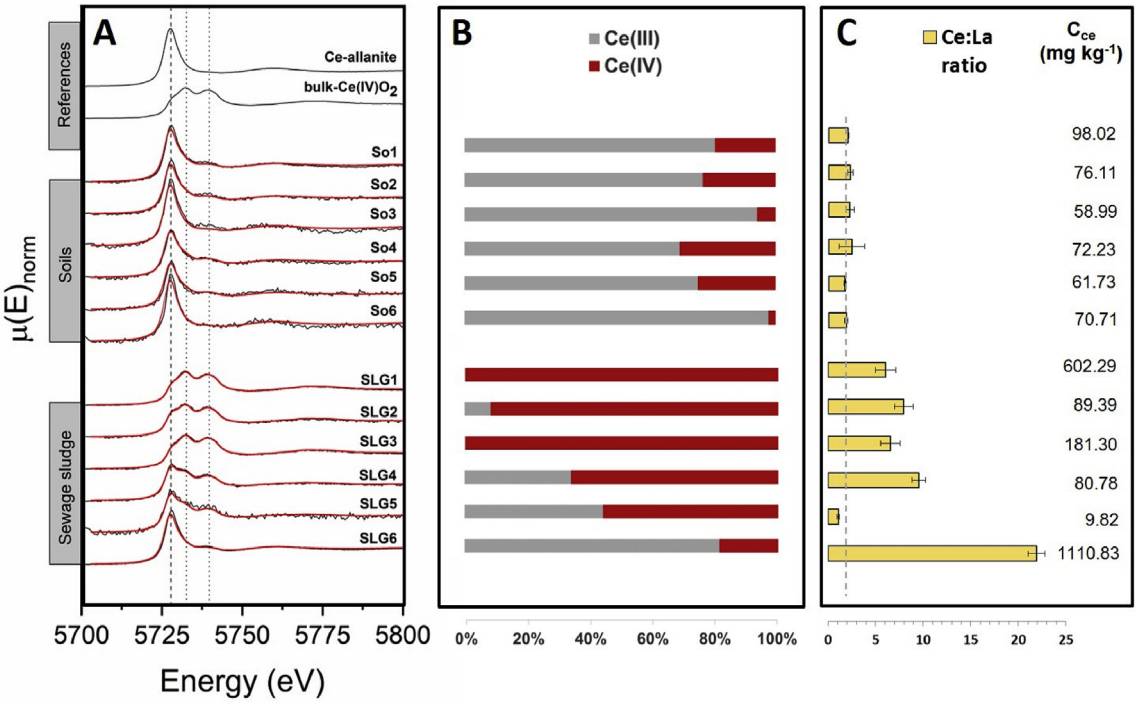

Fig. 1. (A) Normalized Ce L_{III}-edge XANES spectra of soils (So1-6) and sewage sludges (SLG1-6). Vertical lines indicate characteristic XANES features of Ce(IV) (dotted) and Ce(III) (dashed). Ce(III)-allanite and bulk-Ce(IV)O_2 were used as references for Ce(III) and Ce(IV) in the LCF analysis (LCF spectra shown in red). (B) LCF-derived Ce redox speciation. (C) Ce:La ratios in soils and sludges. Error bars were obtained from error propagation of the individual Ce and La relative standard deviations after $\frac{\Delta r}{r} = \frac{\Delta c_{Ce}}{c_{Ce}} + \frac{\Delta c_{La}}{c_{La}}$, where r is the Ce:La ratio and c_{Ce} and c_{La} are the respective element concentrations. The dashed line highlights a Ce:La ratio of 2. Next to the Ce:La ratios, also the absolute Ce concentrations of the respective sample is indicated in mg kg^{-1} (see also Table S3). (For interpretation of the references to colour in this figure legend, the reader is referred to the Web version of this article.)

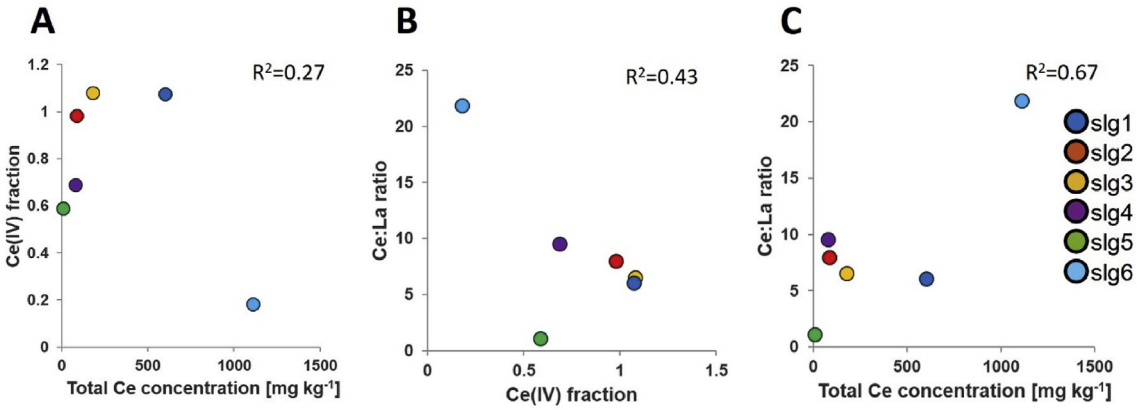

Fig. 2. Total Ce concentration in the sewage sludges versus Ce(IV) fraction (A) and Ce:La ratio (C). Ce(IV) fraction versus Ce:La ratio (B). The correlation factor R^2 shown for each graph was determined from linear regression to the data.

very similar to each other and closely resembled the REE pattern of PAAS (Fig. 3 A), with PAAS-normalized values from ≈0.8–1.0.

In the sewage sludge samples, the REE contents showed a much higher variability and different degrees of enrichment or attenuation relative to PAAS (Fig. 3 B and C). The medium to heavy REE (Eu, Dy, Er) showed consistently lower concentrations relative to the PAAS (PAAS-normalized values of ≈0.1–0.3), reflecting their dilution in organic matter and other sludge components and resulting in correspondingly flat PAAS-normalized REE patterns. For SLG5, the REE pattern also including Ce and La was very comparable to the REE pattern of PAAS, although shifted to lower concentrations. In general agreement with these observations (Kawasaki et al., 1998), reported shale/crust normalized values of ≈0.1–0.6 for 14 different sewage sludges, with rather flat normalized REE patterns for most sludge samples. One sludge however showed higher normalized values for La and Ce (0.45 and 0.6, respectively), which was attributed to elevated concentrations of these elements in the wastewater. Sludge investigated by Suanon et al. (2017) also revealed crust normalized REE ratios smaller than 0.6 in different digested sludges from the US (Verplanck et al., 2010), and PAAS-normalized REE-patterns appeared flat without any pronounced Ce enrichments. Therefore, the consistently flat REE patterns, especially reported for the medium to heavy REE indicated that the concentrations of these elements in sewage sludge were less likely

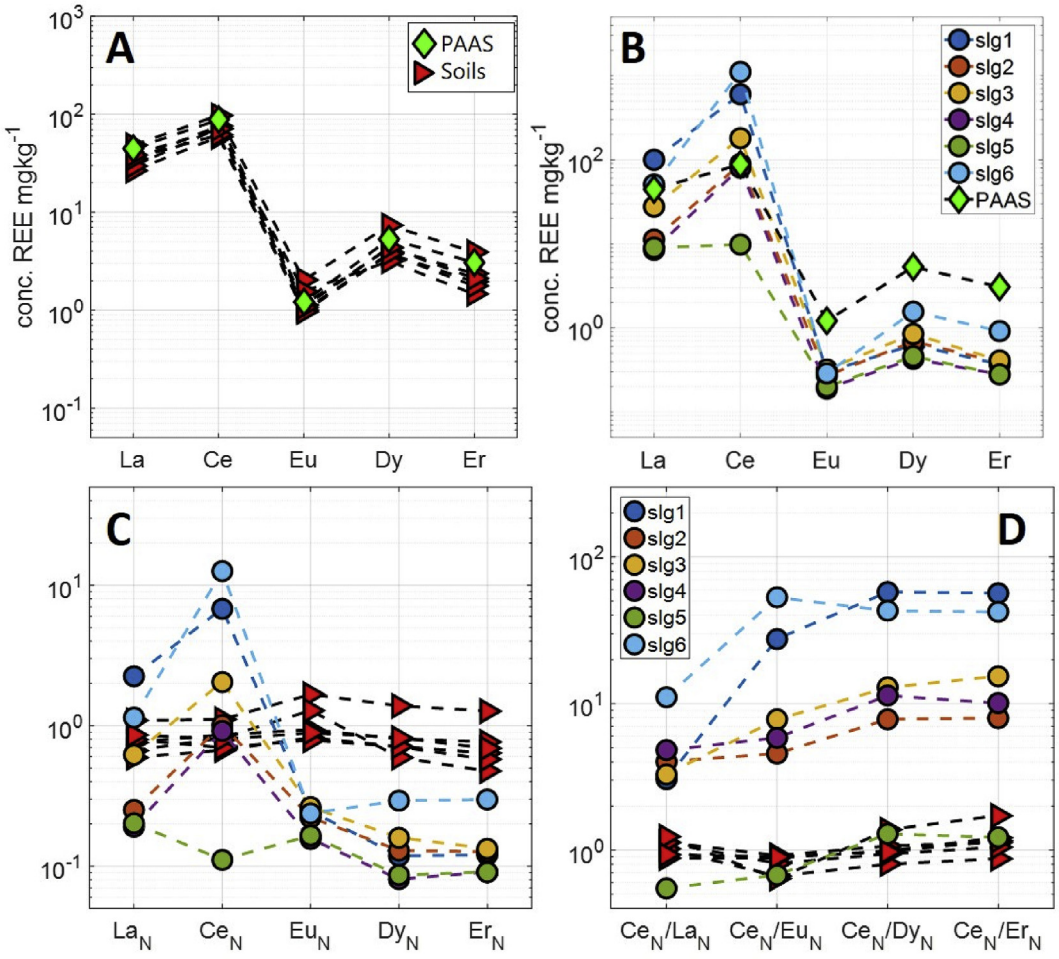

Fig. 3. Rare earth element (REE) concentrations of Post-Archean Australian Shale (PAAS, obtained from Pourmand et al. (2012), green diamonds) and the soils (red triangles) (A) as well as the sludges (B) investigated in this study. REE patterns (REE normalized to PAAS ($\frac{REE_{sample}}{REE_{PAAS}}$)) determined for the soils and for the sewage sludge samples (C). PAAS normalized Ce:REE ratios ($\frac{Ce_{sample}}{Ce_{PAAS}} : \frac{REE_{sample}}{REE_{PAAS}}$) for the soils and sewage sludges (D). (For interpretation of the references to colour in this figure legend, the reader is referred to the Web version of this article.)

to be influenced by anthropogenic contributions and thus reflect variable fractions of geogenic materials in the sewage sludge.

In contrast to the flat normalized REE patterns reported in the literature for other sludges (including SLG5 from this study), the PAAS-normalized REE patterns of all other sludges except SLG5 revealed a pronounced enrichment of Ce relative to Eu, Dy and Er (Fig. 3 C). As Ce (or other REE)-inputs from a geological source would have increased the normalized REE ratios of the other REE to a comparable extent, resulting in a vertical shift of the REE pattern, this clearly indicates anthropogenic Ce inputs to these sludges. In addition to the high normalized Ce concentrations, high normalized La concentrations were observed for the samples SLG1, 3 and 6 relative to Eu, Dy and Er. This further suggests that the anthropogenic Ce inputs were paralleled by anthropogenic La inputs (Fig. 3 C) in these sludges.

The sludge samples SLG2 and SLG4 showed Ce concentrations comparable to PAAS, but La and the heavier REE were strongly depleted compared to PAAS (Fig. 3 C). With the exception of Ce, the normalized REE patterns were rather flat with a shape comparable to the flat REE patterns observed for the normalized REE patterns from the soil samples. This suggests that SLG2 and SLG4 received Ce from anthropogenic applications with negligible contributions of other REEs.

The similarity of the REE patterns observed for SLG1 and 6 and their contrasting oxidation states further support the finding that anthropogenic Ce can be present both in the (IV) and (III) oxidation state.

The normalized REE pattern of sludge SLG5 is very different compared to the normalized REE patterns of the other sludges showing a subtle increase from normalized Ce to normalized La instead of a pronounced peak as observed for all other sludge samples (Fig. 3 C). As a variable contribution of geological material can only shift the normalized REE patterns vertically, but cannot cause any intensity variations between the normalized REEs, the higher normalized La values compared to the normalized Ce values may indicate a selective input of La to the wastewater.

The enrichments of Ce relative to the medium to heavy REE ($\frac{Ce_{sample}}{Ce_{PAAS}} : \frac{REE_{sample}}{REE_{PAAS}} = Ce_N : REE_N$) can best be observed based on Fig. 3 D. Soils (red triangles in Fig. 3 D) generally showed values close to one, reflecting their similarity to the PAAS. Assuming that the REE patterns in the sewage sludge were determined by variable inputs of crustal materials and anthropogenic Ce, a selective contribution of anthropogenic Ce will result in a vertical upward shift of the flat line defined by the crustal material and a kink or a change of the slope on this line indicates additional (anthropogenic) sources of the respective REEs (Fig. 3, D). Sludge samples SLG1 – SLG4 and SLG6 showed a considerable enrichment of normalized Ce relative to the other normalized REEs, reflected by the vertical shift of the

normalized REE patterns in Fig. 3 D. Only the normalized REE ratios of SLG5 remain close to the line defined by the soil samples, therefore suggesting that Ce in this sludge is dominantly geogenic. The clear kink in the Ce_N:La_N for SLG1, 6 and to a lesser extent also for SLG3 reflects an additional La source (Fig. 3 D), as already discussed for the PAAS normalized REE patterns (Fig. 3 C).

For the other sludge samples SLG2, SLG4 and SLG5, only a slight drop at the Ce_N:La_N can be observed, which therefore suggests only a very limited contribution of anthropogenic La. Nevertheless, the Ce_N:La_N of ≈0.55 for sludge SLG5 is clearly smaller than the Ce_N:La_N observed for both the other sludge samples (ratios > 1) and the soil samples (ratios ≈ 1, Fig. 3 D), which is worth noting. As the normalized ratios of Ce to the other REE (Eu, Dy, Er) for this sample were very comparable to the average Ce_N:REE_N observed in the soil samples, this may suggest a specific input of La, as already discussed based on Fig. 3 C. However, considering the uncertainties and assumptions behind these data interpretations, and most importantly, the invariant REE patterns of the background, such small differences have to be treated with great care.

3.5. Quantifying anthropogenic Ce fractions associated with industrial applications in sewage sludge

The ratio of REE to Ce in the sludge samples ($(\frac{REE}{Ce})^{SLG}$) can be calculated based on the sum of the ratios of REE to Ce in the soils (geogenic background, index g) ($(\frac{REE}{Ce})^{g}$) and in anthropogenic sources (index a) ($(\frac{REE}{Ce})^{a}$) weighted by the respective mass fractions (f^{g}_{SLG}, f^{a}_{SLG}) (eq (1)):

$$(\frac{REE}{Ce})^{SLG} = f^{g}_{SLG} \cdot (\frac{REE}{Ce})^{g} + f^{a}_{SLG} \cdot (\frac{REE}{Ce})^{a} \quad (1)$$

Assuming a constant $(\frac{REE}{Ce})^{g}$ ratio in soils, as suggested based on the REE patterns of several soils investigated, and negligible contents of other REE in the anthropogenic Ce-particles ($(\frac{REE}{Ce})^{a} = 0$), the geogenic component in the sludge samples (f^{g}_{SLG}) can be calculated using eqs (2) and (3):

$$f^{g}_{SLG} = \frac{(\frac{REE}{Ce})^{SLG}}{(\frac{REE}{Ce})^{g}} \quad (2)$$

$$f^{a}_{SLG} + f^{g}_{SLG} = 1 \quad (3)$$

Consistently high fractions of anthropogenic Ce were obtained for sludges SLG1 − SLG4 (Fig. 4). The fractions derived from the Eu, Dy and Er ratios ranging from 80 to 100% were in excellent agreement with each other. The fractions derived from the La:Ce ratio were always lower compared to the fractions derived from the other REE ratios. As discussed based on the REE patterns, this likely reflects an additional input of La not necessarily associated with Ce, resulting in an increased La:Ce ratio. Following our quantification scheme, an increased La:Ce ratio in the sewage sludge is directly translating into an increasing fraction of geogenic Ce and concomitantly into a decreasing fraction of anthropogenic Ce. The fractions of anthropogenic Ce obtained for sludge SLG5 were considerably lower as compared to the fraction obtained for the other sludge samples. It has to be mentioned that the La:Ce and Eu:Ce ratios were below the respective ratios determined for the background soil resulting in even negative fractions of anthropogenic Ce and the respective fraction were thus set to 0.

Based on these findings, we conclude that the most robust and reliable estimate of the fraction of anthropogenic Ce in wastewater systems can be derived from Ce:REE ratios of rarely used REE, excluding Ce:La ratios because La very likely has additional inputs from anthropogenic sources. For the investigated sludge samples, generally high anthropogenic fractions of close to 100% were obtained, but also sewage sludge with dominantly geogenic contributions of Ce was observed.

3.6. Morphological characteristics of Ce-containing particles in sewage sludge

To evaluate the morphology and size range of Ce-bearing particles, analytical electron microscopy analyses were conducted on sludge SLG1 with an anthropogenic Ce fraction of close to 100%.

Ce-containing particles observed in the sludge generally

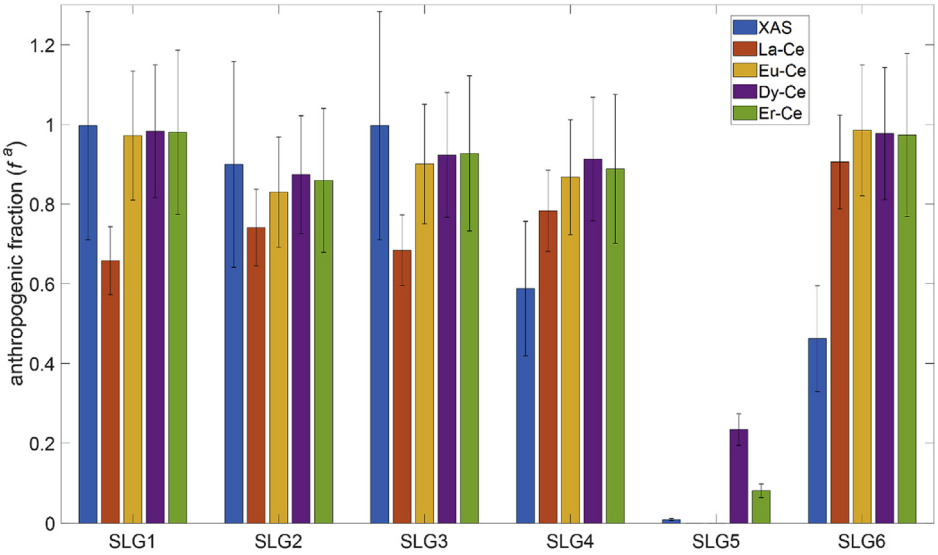

Fig. 4. Fractions of anthropogenic/engineered (ENG) Ce in the different sludge samples derived from the Ce(VI)/Ce(III) ratio (XAS), and from the ratios of REE (La, Eu, Dy, Er) to Ce. Errorbars (±1σ) for the REE based quantifications correspond to the standard deviation of the respective REE/Ce ratios measured in the soil samples divided by the respective mean values, which is expected to represent the dominant term for the uncertainty. For the XAS analyses, an additional uncertainty of 15% associated with the determination of the oxidation state based on XAS LCF analyses is included.

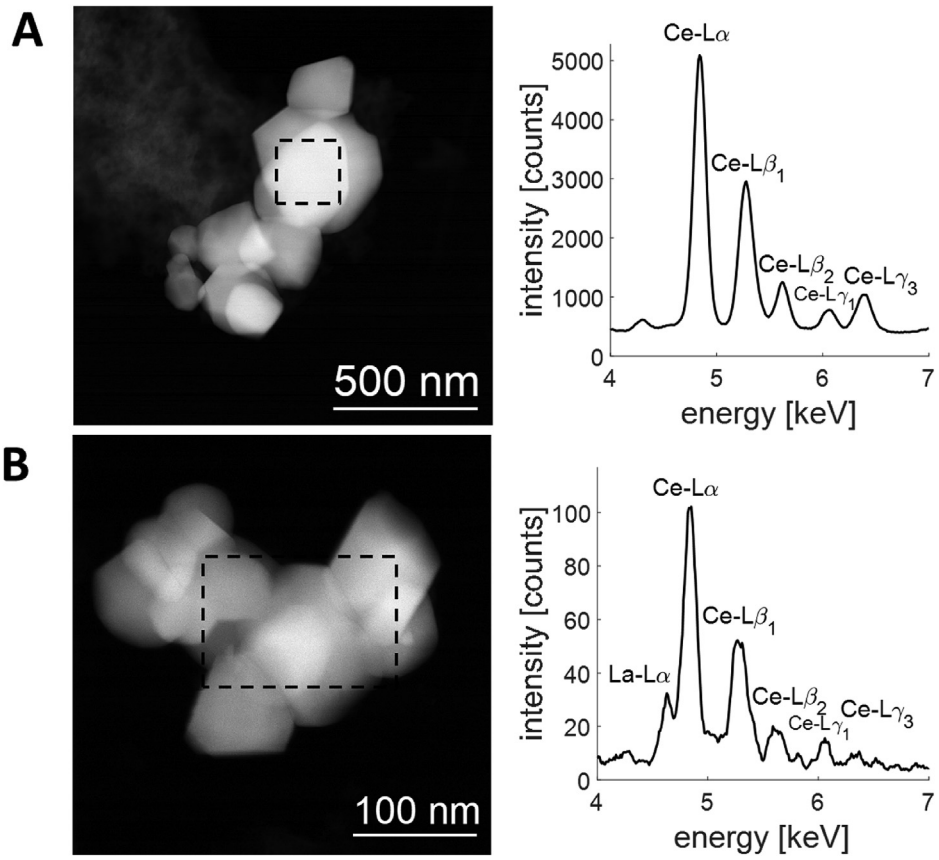

Fig. 5. STEM HAADF micrographs (left) of Ce-containing (nano-)particles observed in sewage sludge and corresponding EDX spectra collected from the areas of the particle as indicated by the dashed rectangles are shown in the right panel.

showed idiomorphically shaped crystals with sharp edges (Fig. 5). Some particles were free of REE other than Ce and additional elements expected for Ce-bearing minerals, such as P (monazite) or Al and Si (Ce-allanite) were only present in minor amounts (Fig. 5 A). These particles are therefore likely representing CeO_2 nanoparticles of anthropogenic origin. However, also particles of supposedly geogenic origin were observed, for example the particle in Fig. 5 B containing La and considerable amounts of F, suggesting that the particle is a bastnaesite particle (Fig. 5 B and Fig. S3). Irrespective of their notional origin, the majority of the Ce-bearing particles observed in the sludge would be classified as nanomaterials, following the EU recommendation (Commission recommendation on the definition of nanomaterial, 2011).

4. Conclusions

Our results show that the determination of multiple REE and Ce/REE ratios allows for a robust quantification of engineered Ce fractions in sewage sludge. In contrast, estimates based on Ce oxidation state are unreliable because the oxidation state of both anthropogenic and natural Ce is variable, and the use of Ce:La ratios is limited because of La accumulation in sewage sludge possibly from additional anthropogenic La inputs. In fact, based on the analysis of full REE patterns, not only industrial Ce fractions, but also industrial fractions of other REE may be readily detectable. Although the results from the electron microscopy are only of qualitative nature and a particle size distribution cannot be extracted from the data, our observations suggest that the majority of anthropogenic Ce seems to fall into the nanosize range. Thus, the anthropogenic fraction derived from REE patterns might serve as a first estimate for the input of engineered CeO_2-NP into wastewater systems and may thus be used to 'validate' current mass-flow models for CeO_2 NP (Giese et al., 2018).

Declaration of competing interest

The authors declare that they have no known competing financial interests or personal relationships that could have appeared to influence the work reported in this paper.

Acknowledgements

We acknowledge the Scientific Center for Optical and Electron Microscopy (ScopeM) of the ETH Zurich for providing access to their microscopes. The Swiss Light Source (SLS, Villigen, Switzerland) is acknowledged for the allocation of beamtime. We thank Maarten Nachtegaal and Olga Safonova for their support at the X10DA beamline. We also kindly acknowledge Brian Sinnet and Matthias Philipp for their support in the laboratory.

Furthermore, we acknowledge Thomas Müntener (ARA Buchs) and Sandra Weber (ProRheno AG Basel) for the possibility to collect samples from the respective WWTP and Andreas Gubler as well as Daniel Wächter (Agroscope, Switzerland) for the provision of the soil samples from the Swiss National Soil Monitoring Network (NABO). This work was undertaken as part of the NanoFASE project receiving funding from the European Union's Horizon 2020 research and innovation programme under grant agreement No 646002.

Appendix A. Supplementary data

Supplementary data to this article can be found online at https://doi.org/10.1016/j.wroa.2020.100059.

References

Commission recommendation on the definition of nanomaterial, 2011. https://eur-lex.europa.eu/legal-content/EN/TXT/?uri=CELEX:32011H0696. Accessed 24.02.2020.

Dahle, J.T., Arai, Y., 2015. Environmental geochemistry of cerium: applications and toxicology of cerium oxide nanoparticles. Int. J. Environ. Res. Publ. Health 12 (2), 1253–1278.

Darab, J.G., Li, H., Vienna, J.D., 1998. X-ray absorption spectroscopic investigation of the environment of cerium in glasses based on complex cerium alkali borosilicate compositions. J. Non-Cryst. Solids 226 (1–2), 162–174.

Desaules, A., Schwab, P., Keller, A., Ammann, S., Paul, J., Bachmann, H., 2006. Anorganische Schadstoffgehalte in Böden der Schweiz und Veränderungen nach 10 Jahren-Ergebnisse der Nationalen Bodenbeobachtung 1985-1999. Agroscope FAL Reckenholz, Eidg. Forschungsanstalt für Agrarökologie und Landbau (Zürich).

Giese, B., Klaessig, F., Park, B., Kaegi, R., Steinfeldt, M., Wigger, H., Gleich, A., Gottschalk, F., 2018. Risks, release and concentrations of engineered nanomaterial in the environment. Sci. Rep. 8 (1), 1565.

Gogos, A., Wielinski, J., Voegelin, A., Emerich, H., Kaegi, R., 2019. Transformation of cerium dioxide nanoparticles during sewage sludge incineration. Environ. Sci. J. Integr. Environ. Res.: Nano 6 (6), 1765–1776.

Haque, N., Hughes, A., Lim, S., Vernon, C., 2014. Rare earth elements: overview of mining, mineralogy, uses, sustainability and environmental impact. Resources 3 (4), 614–635.

Henderson, P., 2013. Rare Earth Element Geochemistry. Elsevier.

Kabata-Pendias, A., 2010. Trace Elements in Soils and Plants. CRC press.

Kawasaki, A., Kimura, R., Arai, S., 1998. Rare earth elements and other trace elements in wastewater treatment sludges. Soil Sci. Plant Nutr. 44 (3), 433–441.

Kulaksız, S., Bau, M., 2011. Rare earth elements in the Rhine River, Germany: first case of anthropogenic lanthanum as a dissolved microcontaminant in the hydrosphere. Environ. Int. 37 (5), 973–979.

Laycock, A., Coles, B., Kreissig, K., Rehkämper, M., 2016. High precision 142 Ce/140 Ce stable isotope measurements of purified materials with a focus on CeO 2 nanoparticles. J. Anal. Atomic Spectrom. 31 (1), 297–302.

Marcus, M.A., Toner, B.M., Takahashi, Y., 2018. Forms and distribution of Ce in a ferromanganese nodule. Mar. Chem. 202, 58–66.

Martin, M., Lin, B., Del Castillo, B., 1988. The use of fluorescent probes in pharmaceutical analysis. J. Pharmaceut. Biomed. Anal. 6 (6–8), 573–583.

Merten, D., Büchel, G., 2004. Determination of rare earth elements in acid mine drainage by inductively coupled plasma mass spectrometry. Microchimica Acta 148 (3–4), 163–170.

Swiss Soil Monitoring Network (Nabo), 2019. https://www.agroscope.admin.ch/agroscope/en/home/topics/environment-resources/soil-bodies-water-nutrients/nabo.html. Accessed 10.03.2020.

Pourmand, A., Dauphas, N., Ireland, T.J., 2012. A novel extraction chromatography and MC-ICP-MS technique for rapid analysis of REE, Sc and Y: revising CI-chondrite and Post-Archean Australian Shale (PAAS) abundances. Chem. Geol. 291, 38–54.

Praetorius, A., Gundlach-Graham, A., Goldberg, E., Fabienke, W., Navratilova, J., Gondikas, A., Kaegi, R., Günther, D., Hofmann, T., von der Kammer, F., 2017. Single-particle multi-element fingerprinting (spMEF) using inductively-coupled plasma time-of-flight mass spectrometry (ICP-TOFMS) to identify engineered nanoparticles against the elevated natural background in soils. Environ. Sci. J. Integr. Environ. Res.: Nano 4 (2), 307–314.

Schreiber, H.D., Lauer Jr., H.V., Thanyasiri, T., 1980. The redox state of cerium in basaltic magmas: an experimental study of iron-cerium interactions in silicate melts. Geochem. Cosmochim. Acta 44 (10), 1599–1612.

Suanon, F., Sun, Q., Yang, X., Chi, Q., Mulla, S.I., Mama, D., Yu, C.-P., 2017. Assessment of the occurrence, spatiotemporal variations and geoaccumulation of fifty-two inorganic elements in sewage sludge: a sludge management revisit. Sci. Rep. 7 (1), 5698.

Takahashi, Y., Shimizu, H., Usui, A., Kagi, H., Nomura, M., 2000. Direct observation of tetravalent cerium in ferromanganese nodules and crusts by X-ray-absorption near-edge structure (XANES). Geochem. Cosmochim. Acta 64 (17), 2929–2935.

Takahashi, Y., Sakami, H., Nomura, M., 2002. Determination of the oxidation state of cerium in rocks by Ce LIII-edge X-ray absorption near-edge structure spectroscopy. Anal. Chim. Acta 468 (2), 345–354.

Takahashi, Y., Yuita, K., Kihou, N., Shimizu, H., Nomura, M., 2005. Determination of the Ce (IV)/Ce (III) ratio by XANES in soil horizons and its comparison with the degree of Ce anomaly. Phys. Scripta 2005 (T115), 936.

Verplanck, P.L., Furlong, E.T., Gray, J.L., Phillips, P.J., Wolf, R.E., Esposito, K., 2010. Evaluating the behavior of gadolinium and other rare earth elements through large metropolitan sewage treatment plants. Environ. Sci. Technol. 44 (10), 3876–3882.

Vivian, C., 1986. Rare earth element content of sewage sludges dumped at sea in Liverpool Bay, UK. Environ. Technol. 7 (1–12), 593–596.

Voncken, J.H.L., 2016. The Rare Earth Elements: an Introduction. Springer.

Vriens, B., Voegelin, A., Hug, S.J., Kaegi, R., Winkel, L.H., Buser, A.M., Berg, M., 2017. Quantification of element fluxes in wastewaters: a nationwide survey in Switzerland. Environ. Sci. Technol. 51 (19), 10943–10953.

Webb, S., 2005. SIXpack: a graphical user interface for XAS analysis using IFEFFIT. Phys. Scripta 2005 (T115), 1011.